JOURNAL OF BACTERIOLOGY, Mar. 2008, p. 1871–1878 Vol. 190, No. 6
0021-9193/08/$08.00+0 doi:10.1128/JB.01616-07

Role of Periplasmic Trehalase in Uptake of Trehalose by the Thermophilic Bacterium *Rhodothermus marinus*▽

Carla D. Jorge,[1] Luís L. Fonseca,[1] Winfried Boos,[2] and Helena Santos[1]*

Instituto de Tecnologia Química e Biológica, Universidade Nova de Lisboa, Rua da Quinta Grande 6, Apartado 127, 2780-156 Oeiras, Portugal,[1] and Department of Biology, University of Konstanz, D-78434 Konstanz, Germany[2]

Received 4 October 2007/Accepted 23 December 2007

Trehalose uptake at 65°C in *Rhodothermus marinus* was characterized. The profile of trehalose uptake as a function of concentration showed two distinct types of saturation kinetics, and the analysis of the data was complicated by the activity of a periplasmic trehalase. The kinetic parameters of this enzyme determined in whole cells were as follows: K_m = 156 ± 11 μM and V_{max} = 21.2 ± 0.4 nmol/min/mg of total protein. Therefore, trehalose could be acted upon by this periplasmic activity, yielding glucose that subsequently entered the cell via the glucose uptake system, which was also characterized. To distinguish the several contributions in this intricate system, a mathematical model was developed that took into account the experimental kinetic parameters for trehalase, trehalose transport, glucose transport, competition data with trehalose, glucose, and palatinose, and measurements of glucose diffusion out of the periplasm. It was concluded that *R. marinus* has distinct transport systems for trehalose and glucose; moreover, the experimental data fit perfectly with a model considering a high-affinity, low-capacity transport system for trehalose (K_m = 0.11 ± 0.03 μM and V_{max} = 0.39 ± 0.02 nmol/min/mg of protein) and a glucose transporter with moderate affinity and capacity (K_m = 46 ± 3 μM and V_{max} = 48 ± 1 nmol/min/mg of protein). The contribution of the trehalose transporter is important only in trehalose-poor environments (trehalose concentrations up to 6 μM); at higher concentrations trehalose is assimilated primarily via trehalase and the glucose transport system. Trehalose uptake was constitutive, but the activity decreased 60% in response to osmotic stress. The nature of the trehalose transporter and the physiological relevance of these findings are discussed.

Trehalose [α-D-glucopyranosyl-α(1,1)-D-glucopyranoside] is a nonreducing disaccharide that is widespread in the three domains of life. This sugar often accumulates intracellularly and protects against a variety of stresses (4, 17). Given the ubiquitous distribution of trehalose in all types of biotopes, it is not surprising that efficient systems for uptake of this sugar evolved in many organisms. In particular, several mechanisms have been discovered in prokaryotes and studied to different extents. In mesophilic bacteria, like *Escherichia coli*, the uptake of trehalose is typically mediated by the phosphoenolpyruvate (PEP):sugar phosphotransferase system (PTS) (2). In contrast, the PTS has not been found in extreme thermophiles or hyperthermophiles, and the ATP-binding cassette (ABC) transport system is used for trehalose uptake in the few cases examined thus far (5, 9, 18, 24, 25). The high affinity of the ABC transporters seems to be crucial for utilization of the scarce carbon sources typical of the hostile environments where thermophiles and hyperthermophiles are found.

Rhodothermus marinus is a thermophilic bacterium with an optimal growth temperature of 65°C, and it was isolated from marine hot springs in the Azores Islands (1). In response to heat or osmotic stress, *R. marinus* accumulates mannosylglycerate and mannosylglyceramide as major compatible solutes, but minor amounts of glucose and trehalose are also present (19). Mannosylglycerate is commonly found in thermophilic and hyperthermophilic bacteria and archaea that colonize hot marine environments, while mannosylglyceramide has been found only in members of the genus *Rhodothermus* (16). In response to stress, compatible solutes can be synthesized de novo or, when they are available, taken up from the medium. Therefore, we set out to study the transport of compatible solutes in *R. marinus* as part of our effort to elucidate strategies of osmo- and thermoadaptation in thermophiles and hyperthermophiles. This bacterium was unable to take up mannosylglycerate (15), but trehalose was transported efficiently. However, the presence of a very active trehalase in the periplasmic space (10) complicated characterization of the transport properties. The first question that arose is whether there is an independent transporter for trehalose or whether this sugar is fully acted upon by trehalase, with the resulting glucose internalized via a specific transport system. Moreover, possible diffusion of glucose out of the periplasmic space has to be considered. The complexity of this system demanded the development of a mathematical model that was used to interpret the experimental data. In the present study, the transport of trehalose and glucose in *R. marinus* was thoroughly characterized, and the role of the periplasmic trehalase in the uptake of trehalose was clarified.

MATERIALS AND METHODS

^{14}C-labeled compounds. For transport assays, [U-^{14}C]glucose (Amersham) and [U-^{14}C]trehalose (Trenzyme) with specific activities of 290 and 660 mCi/mmol, respectively, were used.

Bacterial strain and growth conditions. *R. marinus* strain DSM 4252^T was obtained from the Deutsche Sammlung von Mikroorganismen und Zellkulturen

* Corresponding author. Mailing address: Instituto Tecnologia Química e Biológica/UNL, Rua da Quinta Grande 6, 2780-156 Oeiras, Portugal. Phone: 351 21 4469800. Fax: 351 21 4428766. E-mail: santos@itqb.unl.pt.

▽ Published ahead of print on 11 January 2008.

GmbH, Braunschweig, Germany. Cultures of *R. marinus* were grown on Degryse 162 medium, as modified by Nunes et al. (13), containing (per liter) 2.5 g tryptone, 2.5 g yeast extract, and 10 g (or 40 g) NaCl, or in trehalose-free (TF) medium, which contained (per liter) the basal salts of Degryse 162 medium, 2.5 g tryptone, 10 g NaCl, 3.5 mg tyrosine, 3.5 mg cysteine, and 10 ml of a vitamin solution having a concentration of 4 mg/liter (20). Yeast extract was not used in this medium since it contained trehalose. Thin-layer chromatography (TLC) and proton nuclear magnetic resonance analysis confirmed the absence of trehalose in tryptone (Difco). To study the expression of the trehalose transport in *R. marinus*, cells were grown in TF medium supplemented with trehalose or glucose (final concentration, 2 mM). Cell growth was monitored by measuring the turbidity at 600 nm.

Transport assays in whole cells. *R. marinus* cells were grown to mid-exponential phase (optical density at 600 nm [OD_{600}], 1), harvested by centrifugation (6,000 × *g*, 20°C, 10 min), and washed twice with 50 mM phosphate buffer (pH 6.5) containing 10 g (or 40 g) NaCl per liter (buffer A). The cells were suspended in buffer A to a final OD_{600} of 0.5 or 1 and kept at room temperature. Under these conditions, it was verified that cells maintained their transport capabilities for 2 h after centrifugation. In all transport assays, the cell suspension was prewarmed at 65°C for 2 min before addition of the radiolabeled sugar. For trehalose uptake measurements, 2 ml of a cell suspension (OD_{600}, 0.5) was incubated at 65°C, and the assays were started by addition of [^{14}C]trehalose. Depending on the desired final trehalose concentration, different concentrations of [^{14}C]trehalose were used: 54 nM [^{14}C]trehalose for total trehalose concentrations up to 2 μM; 0.5 μM [^{14}C]trehalose for concentrations ranging from 5 to 50 μM; and 0.8 μM [^{14}C]trehalose for concentrations up to 400 μM. At trehalose concentrations higher than 150 μM, cell suspensions with a final OD_{600} of 1 were used to counterbalance the reduction in the final concentration of labeled trehalose. Aliquots were removed at different time points, filtered through nitrocellulose filters (pore size, 0.45 μm; Millipore), and washed with buffer A. The radioactivity retained on the filters was counted in a toluene-based scintillation fluid.

Glucose transport assays were carried out by using a similar procedure; 1.7 ml of a cell suspension (OD_{600}, 0.5) was preheated at 65°C, and the assays were initiated by addition of [^{14}C]glucose to obtain a final concentration of labeled sugar of 1.5 μM. Higher glucose concentrations (up to 400 μM) were obtained by addition of unlabeled glucose. At different time points aliquots were removed and filtered, and the radioactivity was counted as described above.

Rates of transport of trehalose (final concentrations, 0.05 to 1.5 μM) were also determined in the presence of 100 μM glucose in order to calculate the apparent inhibition constant (K_i) of glucose for trehalose transport. A similar experiment was performed to assess the apparent inhibition constant of palatinose for glucose transport; the uptake of glucose (final concentration, 1.5 to 400 μM) was measured in the presence of 7.5 mM palatinose.

In transport competition assays, cell suspensions (OD_{600}, 0.5) were incubated with trehalose at a final concentrations of 1 and 50 μM, 0.2 and 0.5 μM of which consisted of [^{14}C]trehalose, respectively. The initial rates of sugar uptake were measured in the presence of the following unlabeled carbohydrates at final concentrations of 1 and 2 mM, respectively: trehalose, glucose, α-methyl-glucopyranoside, maltose, maltotriose, sucrose, palatinose, and fructose. Linear correlations for the number of counts versus time were obtained (correlation coefficient, at least 0.98). Similar competition assays were carried out to evaluate the effects of different carbohydrates (final concentration, 2 mM) on the uptake of 2 μM [^{14}C]glucose.

The presence of an active trehalase in the periplasm of *R. marinus* creates an unavoidable link between trehalose transport and glucose transport, as the supply of trehalose necessarily produces glucose. Therefore, the following experiments were designed to characterize this convoluted behavior: (i) the uptake of 50 μM trehalose (0.5 μM of which was radioactive) was measured in the presence of the same concentration (50 μM) of unlabeled glucose; and (ii) the uptake of 50 μM glucose (1.5 μM of which was radioactive) was measured in the presence of the same concentration of unlabeled trehalose (50 μM). Similar assays were carried out in the presence of 7.5 mM palatinose to study the influence of palatinose on the uptake of trehalose and glucose.

To determine whether the trehalose transport system was induced by trehalose or glucose in the growth medium, the rates of uptake of trehalose (final concentrations, 2 and 250 μM) were measured in cells grown in TF medium or in TF medium supplemented with 2 mM trehalose or 2 mM glucose.

Effects of inhibitors on the uptake of trehalose and glucose. Transport of trehalose and glucose was measured using cell suspensions (2 ml; OD_{600}, 0.5) containing carbonyl cyanide *m*-chlorophenylhydrazone (CCCP) (140 μM), sodium arsenate (45 mM), or sodium fluoride (28 mM). The assays were initiated by adding [^{14}C]trehalose (final concentration, 0.08 μM) or [^{14}C]glucose (final concentration, 0.9 μM). The influence of ethanol on the uptake of trehalose and glucose was also examined, since CCCP was dissolved in this solvent.

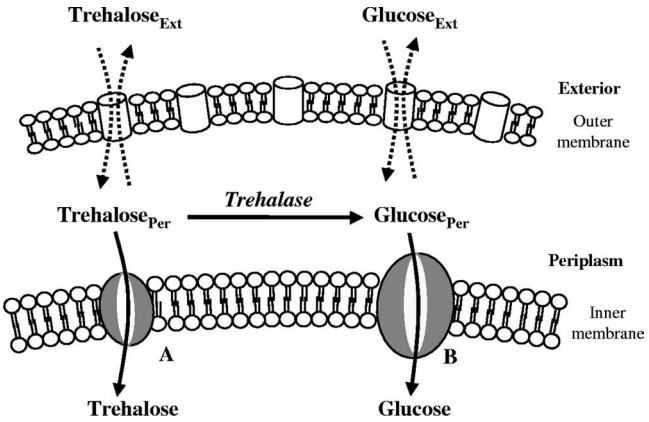

FIG. 1. Schematic diagram of the model proposed for trehalose transport in *R. marinus*. Trehalose can be taken up by two pathways: a high-affinity trehalose transport system (A) and via trehalase and subsequent internalization of the resulting glucose by the glucose transport system (B). Ext, exterior; Per, periplasm.

Internalization of trehalose and glucose. Assays were initiated by adding 0.32 μM [^{14}C]trehalose or 0.16 μM [^{14}C]glucose to 1 ml of a cell suspension (OD_{600}, 0.5) prewarmed at 65°C. After 30, 60, or 120 s each mixture was centrifuged (15 s), the radioactivity present in the supernatant was quantified, and the cell pellet was extracted with trichloroacetic acid (4°C, 10 min). The extract was centrifuged, and the supernatant was applied to TLC plates (Silica Gel 60; Merck). The chromatograms were developed with a solvent system consisting of butanol, ethanol, and water (5:3:2, vol/vol/vol), and the positions of radioactive compounds were visualized by autoradiography.

Trehalase activity in whole cells. We found that addition of CCCP (final concentration, 140 μM) eliminated the uptake of trehalose and glucose. Therefore, the assays to determine trehalase activity were carried out in the presence of this protonophore, using two different approaches. In the radioactive method, a cell suspension (OD_{600}, 0.5) was preheated at 65°C and subsequently incubated with CCCP for 1 min at the same temperature. The assay was started by adding 0.9 μM [^{14}C]trehalose plus different concentrations of unlabeled trehalose (final concentrations, 0.03 to 0.5 mM). At appropriate time points, aliquots were removed and immediately frozen in liquid nitrogen. Supernatants obtained after centrifugation were applied to TLC plates. The chromatograms were developed with the solvent system described above, and the radioactive glucose formed was quantified on the TLC plates using a Molecular Dynamics PhosphorImager (laser scanner).

In the alternative method, a cell suspension (OD_{600}, 0.5) was incubated with CCCP as described above, and the assays were initiated by adding unlabeled trehalose (final concentration, 0.1 to 5 mM). At different time points, samples were removed and immediately frozen in liquid nitrogen. After centrifugation, the glucose present in the supernatant was quantified using a glucose assay kit (Merck).

Quantification of glucose released from the periplasmic space into the external medium. The assay started by adding 5 mM trehalose to a cell suspension (2 ml; OD_{600}, 0.5). After 30 min of incubation at 65°C, the mixture was immediately frozen in liquid nitrogen. Following centrifugation the concentration of glucose in the supernatant was determined using a glucose assay kit (Merck).

Protein determination. Cells were disrupted in a French press (three treatments at 100 MPa), and the protein content was estimated by the method of Bradford (3), using bovine serum albumin as the standard.

Mathematical model of trehalose uptake. To analyze the uptake of trehalose in *R. marinus*, a mathematical model was developed. The model considered a trehalose transporter, a glucose transporter, and a periplasmic trehalase; moreover, diffusion of trehalose and glucose between the extracellular and periplasmic compartments was taken into account (Fig. 1). The diffusion of trehalose and glucose into and out of the periplasmic space was modeled as following first-order kinetics with the same rate constant for the diffusion of the two molecules. The following equations were used to describe trehalose and glucose uptake:

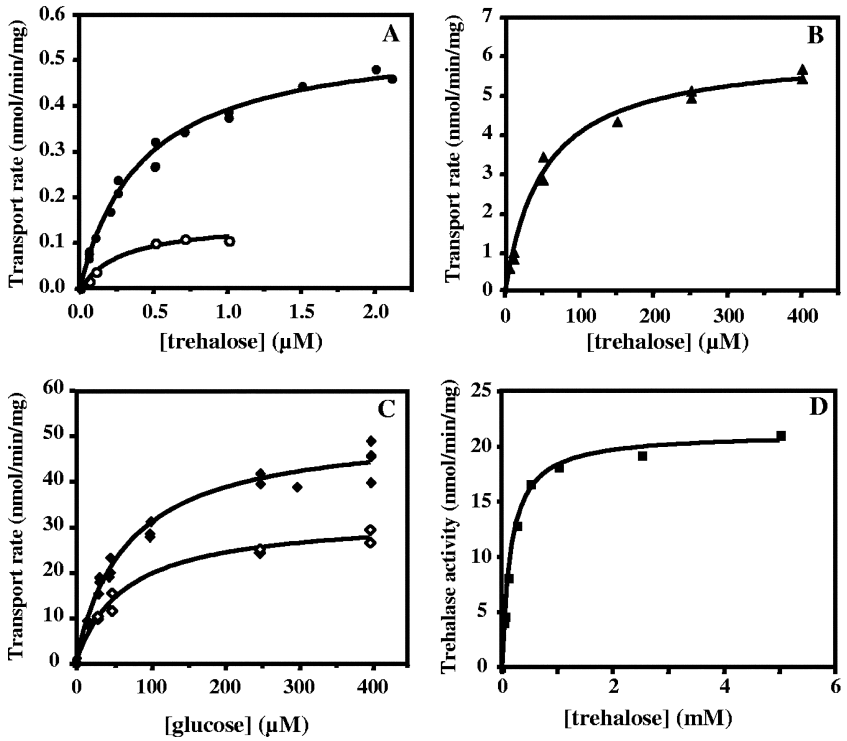

FIG. 2. Determination of apparent K_m and V_{max} values for (A) trehalose transport at low concentrations in the absence (●) or in the presence (○) of 100 μM glucose, (B) trehalose transport at high concentrations (▲), (C) glucose transport in the absence (◆) or in the presence (◇) of 7.5 mM palatinose, and (D) trehalase activity. Trehalase activity is expressed in nmol trehalose hydrolyzed per min per mg of total protein.

$$\frac{d[tre]_{Ext}}{dt} = k \cdot [tre]_{Per} - k \cdot [tre]_{Ext}$$

$$\frac{d[glc]_{Ext}}{dt} = k \cdot [glc]_{Per} - k \cdot [glc]_{Ext}$$

$$\frac{d[tre]_{Per}}{dt} = -k \cdot [tre]_{Per} + k \cdot [tre]_{Ext} - F^{Ttre} - F^{trehalase}$$

$$\frac{d[glc]_{Per}}{dt} = -k \cdot [glc]_{Per} + k \cdot [glc]_{Ext} - F^{Tglc} + 2 \cdot F^{trehalase}$$

where $[tre]_{Ext}$ and $[tre]_{Per}$ are the extracellular and periplasmic concentrations of trehalose, respectively; $[glc]_{Ext}$ and $[glc]_{Per}$ are the extracellular and periplasmic concentrations of glucose, respectively; k is the first-order rate constant for glucose and trehalose exchange through the extracellular membrane; and F^{Ttre}, F^{Tglc}, and $F^{trehalase}$ are the fluxes through the trehalose transporter, the glucose transporter, and the trehalase, respectively. The calculations took into account that the assays were carried out with 2 ml of cell suspension corresponding to 0.326 mg of cell protein; the intracellular volume of *R. marinus* was assumed to be 1.2 μl/mg of protein, a typical value obtained for bacterial rods (26). Moreover, the periplasmic space was assumed to be 30% of the total intracellular space by analogy with the model gram-negative organism *E. coli* (22).

On the basis of the experimental data, both transporters were modeled with Michaelis-Menten kinetics. The trehalose uptake (F^{Ttre}) was modeled as being noncompetitively inhibited by glucose and palatinose, while the glucose uptake (F^{Tglc}) was noncompetitively inhibited by palatinose. The periplasmic trehalase activity ($F^{trehalase}$) was described by Michaelian kinetics with a competitive inhibition constant for glucose of 7 mM (10). The following equations were used to describe these fluxes:

$$F^{Ttre} = \frac{V_{max}^{Ttre}/[(1 + [glc]_{Per}/K_{i,glc}^{Ttre}) \cdot (1 + [pal]/K_{i,pal}^{Ttre})] \cdot [tre]_{Per}}{[tre]_{Per} + K_m^{Ttre}}$$

$$F^{trehalase} = \frac{V_{max}^{trehalase} \cdot [tre]_{Per}}{[tre]_{Per} + K_m^{trehalase} \cdot (1 + [glc]_{Per}/K_{i,glc}^{trehalase})}$$

$$F^{Tglc} = \frac{V_{max}^{Tglc}/(1 + [pal]/K_{i,pal}^{Tglc}) \cdot [glc]_{Per}}{[glc]_{Per} + K_m^{Tglc}}$$

where [pal] is the extracellular concentration of palatinose; V_{max}^{Ttre}, V_{max}^{Tglc}, and $V_{max}^{trehalase}$ are the maximum rates of trehalose transport and glucose transport and maximum trehalase activity, respectively; K_m^{Ttre}, K_m^{Tglc}, and $K_m^{trehalase}$ are the affinity constants for trehalose uptake, glucose uptake, and trehalase, respectively; $K_{i,glc}^{Ttre}$ and $K_{i,pal}^{Ttre}$ are the inhibition constants of glucose and palatinose for trehalose transport, respectively; $K_{i,glc}^{trehalase}$ is the inhibition constant of glucose for trehalase activity; and $K_{i,pal}^{Tglc}$ is the inhibition constant of palatinose for glucose transport.

The model was developed as a set of ordinary differential equations in MATLAB (The MathWorks), which were numerically integrated using the ODE45 solver; the parameters were estimated by fitting the experimental data using the least-squares method (fminsearch function).

RESULTS

Transport of trehalose and glucose in *R. marinus*. An apparent K_m of 0.42 ± 0.04 μM and a V_{max} of 0.56 ± 0.02 nmol/min/mg of protein were determined for the low range of trehalose concentrations (i.e., up to 2 μM) (Fig. 2A); an apparent K_m of 52 ± 5 μM and a V_{max} of 6.1 ± 0.2 nmol/min/mg of protein were determined for higher trehalose concentrations (up to 400 μM) (Fig. 2B); and an apparent K_m of 69 ± 6 μM and a V_{max} of 52 ± 1 nmol/min/mg of protein were determined for glucose uptake (Fig. 2C). These results were obtained with cells grown in medium containing 1% NaCl, but the transport of trehalose (at concentrations up to 2 μM) was also examined in cells grown in medium containing 4% NaCl, which resulted in an apparent K_m of 0.25 ± 0.06 μM and a V_{max} of 0.23 ± 0.02 nmol/min/mg of protein.

Glucose behaved as a noncompetitive inhibitor of trehalose

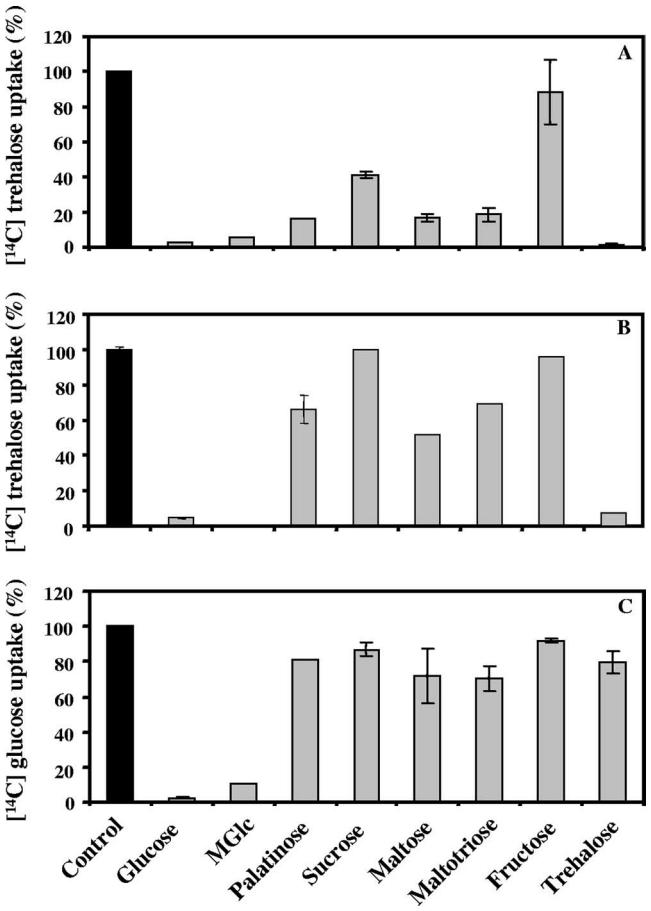

FIG. 3. Effects of competing sugars on (A) the uptake of 1 μM trehalose in the presence of the specified sugars at a concentration of 1 mM, (B) the uptake of 50 μM trehalose in the presence of the specified sugars at a concentration of 2 mM, and (C) the uptake of 2 μM glucose in the presence of the specified sugars at a concentration of 2 mM. The transport rates are expressed as percentages of the control rates; 100% corresponds to 0.6 nmol of [^{14}C]trehalose/min/mg of protein (A), to 3.2 nmol of [^{14}C]trehalose/min/mg of protein (B), and to 2 nmol of [^{14}C]glucose/min/mg of protein (C). Experiments were done in duplicate. The effect of α-methyl-glucopyranoside (MGlc) on the uptake of 50 μM trehalose was not examined.

transport with an apparent K_i of 43 ± 6 μM (Fig. 2A). In the low-concentration range, transport of trehalose was strongly inhibited by an excess of palatinose, maltose, or maltotriose (around 80%) and was virtually eliminated by glucose and α-methyl-glucopyranoside; moreover, it was inhibited by sucrose (60%), and fructose had no effect (Fig. 3A).

The uptake of glucose was inhibited by palatinose in a noncompetitive fashion with an apparent K_i of 14 ± 2 mM (Fig. 2C). Palatinose, sucrose, maltose, maltotriose, fructose, and trehalose inhibited glucose transport to a small extent (less than 40%), while α-methyl-glucopyranoside was a strong inhibitor (Fig. 3C). A similar competition pattern was observed for the uptake of trehalose at higher concentrations (50 μM) (Fig. 3B). These results suggest that the operation of a high-affinity trehalose transporter is distinct from the operation of the glucose transporter. However, in the high range of trehalose concentrations, the picture is complicated by the action of a highly active periplasmic trehalase that hydrolyzes trehalose, yielding glucose. Therefore, it is still not known whether trehalose is taken up as such or is assimilated as glucose via the glucose transporter. To clarify this point, the transport of trehalose was examined in the presence of glucose and/or palatinose, a sugar that differentially inhibits trehalose and glucose uptake. Conversely, the uptake of glucose was examined in the presence of trehalose and/or palatinose. Data from this array of experiments are shown in Table 1.

TABLE 1. Effect of glucose and/or palatinose on the uptake of trehalose and effect of trehalose and/or palatinose on the uptake of glucose in *R. marinus*

Compound(s)	Transport rate (%)[a]
Trehalose (50 μM)	100 ± 12
Trehalose (50 μM) + glucose (50 μM)	91 ± 1
Trehalose (50 μM) + palatinose (7.5 mM)	27 ± 3
Trehalose (50 μM) + glucose (50 μM) + palatinose (7.5 mM)	20 ± 2
Glucose (50 μM)	100 ± 2
Glucose (50 μM) + trehalose (50 μM)	85 ± 5
Glucose (50 μM) + palatinose (7.5 mM)	69 ± 14
Glucose (50 μM) + trehalose (50 μM) + palatinose (7.5 mM)	77 ± 0.1

[a] The transport rates are expressed as percentages of the corresponding control rates; 100% corresponds to a transport rate of 3 nmol of [^{14}C]trehalose/min/mg of protein or 20 nmol of [^{14}C]glucose/min/mg of protein. Experiments were done in duplicate, and the values are the means ± standard errors of the means.

Trehalose was taken up without modification. Further evidence for the presence of an independent trehalose transporter in the low-concentration range was derived from the analysis of trichloroacetic acid extracts of cells incubated with radiolabeled trehalose (Fig. 4A). The detection of labeled trehalose in the intracellular milieu supports the hypothesis that there is a high-affinity transport system that takes up trehalose without modification. The spots assigned to glucose are likely due to the activity of trehalase. Control experiments in which radiolabeled glucose was supplied instead of trehalose ruled out the possibility that intracellular trehalose originated from glucose (Fig. 4B).

Effects of inhibitors on the uptake of trehalose and glucose. To investigate the nature of trehalose and glucose transport systems, the uptake of these sugars was measured in the pres-

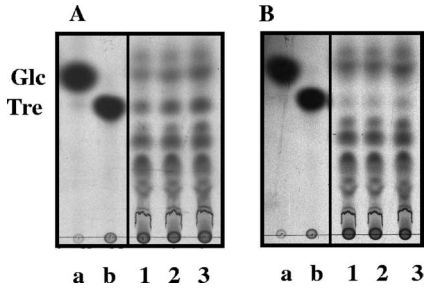

FIG. 4. TLC analysis of radiolabeled compounds after uptake of 0.32 μM [^{14}C]trehalose (A) or 0.16 μM [^{14}C]glucose (B). The standards were [^{14}C]glucose (lane a) and [^{14}C]trehalose (lane b). Lanes 1, 2, and 3, incubation times of 30, 60, and 120 s, respectively.

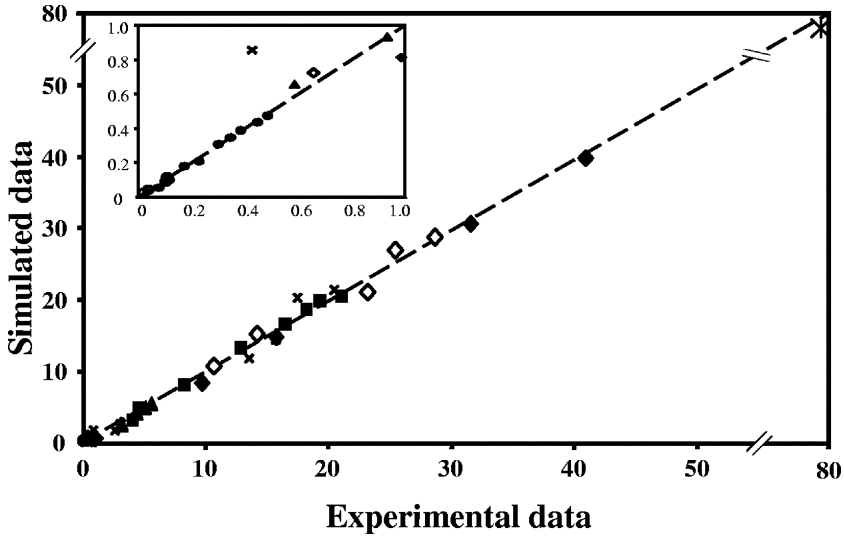

FIG. 5. Model quality test: data for trehalose uptake at low concentrations (●), trehalose uptake in the presence of glucose (○), trehalose uptake at high concentrations (▲), glucose uptake (◇), glucose uptake in the presence of palatinose (◆), trehalase activity (■), effect of trehalose and/or palatinose on the uptake of glucose or effect of glucose and/or palatinose on the uptake of trehalose (×), and glucose diffusion (∗).

ence of known transport inhibitors, including CCCP, a proton uncoupler agent; sodium fluoride, an inhibitor of enolase, which prevents the formation of PEP; and sodium arsenate, an inhibitor of ATP synthesis. The rate of glucose transport was slightly affected by fluoride (10% inhibition) and by arsenate (24% inhibition), but glucose transport was completely eliminated by CCCP. We confirmed that these effects were not due to toxicity of the ethanol used to dissolve the inhibitors. Transport of trehalose (0.08 μM) was moderately inhibited by fluoride (34%), reduced considerably by arsenate (81%), and eliminated by CCCP. These results indicate that the transporters of glucose and trehalose are PEP independent.

Kinetic parameters of trehalase determined with whole cells. The periplasmic trehalase exhibited a K_m of 156 ± 11 μM and a $V_{\max}$ of 21.2 ± 0.4 nmol/min/mg of protein (Fig. 2D). These parameters were measured in the presence of 140 μM CCCP to eliminate trehalose and glucose uptake. The results verified that sodium arsenate (45 mM), CCCP (140 μM), and sodium fluoride (28 mM) did not inhibit the activity of recombinant trehalase (10).

Quantification of glucose diffusing out of the periplasmic space into the external medium. The low capacity for trehalose uptake (around 6 nmol/min/mg of protein) shown in Fig. 2B was puzzling when it was compared to the magnitude of the trehalase activity (21.2 nmol trehalose/min/mg of protein) and the apparent capacity of the glucose transporter (52 nmol/min/mg of protein). It seemed as though most of the glucose derived from trehalose was not taken up by the cells. The hypothesis that a considerable proportion of glucose diffused out of the periplasm was developed to explain these findings. Experimental evidence in support of this hypothesis was obtained by incubating whole cells with 5 mM trehalose and measuring the diffusion of glucose into the extracellular space at different time points up to 30 min. At 30 min the concentration of glucose in the extracellular space was 79.9 ± 1.6 μM.

Induction of trehalose transport. The expression of the trehalose transport system was investigated in cells grown in TF medium supplemented with trehalose. There was no difference between the rates of trehalose transport (final concentrations, 2 and 250 μM) in cells grown in TF medium (0.6 and 6 nmol/min/mg of protein, respectively) and the rates of transport measured in cells grown in the presence of trehalose, indicating that trehalose transport was constitutive. The rate of trehalose transport (final concentration, 2 μM) was also determined in cells grown in TF medium with glucose. The uptake of trehalose was not altered.

Mathematical model. The mathematical model described in Materials and Methods was fitted to the experimental data, which comprised the kinetics of trehalose transport in the absence and presence of glucose (Fig. 2A and 2B), the kinetics of glucose transport in the absence and presence of palatinose (Fig. 2C), and the kinetics of trehalose hydrolysis (Fig. 2D), glucose-releasing assays, transport of trehalose in the presence of glucose and/or palatinose, and transport of glucose in the presence of trehalose and/or palatinose (Table 1). Replicates were averaged to reduce processing time. A total of 51 independent experimental points were used to calculate 10 parameters in the model, including the kinetic constants of glucose and trehalose transporters and trehalase and the first-order rate constant of exchange of glucose and trehalose through the extracellular membrane (V_{max}^{Ttre}, V_{max}^{Tglc}, $V_{max}^{trehalase}$, K_m^{Ttre}, K_m^{Tglc}, $K_m^{trehalase}$, $K_{i,glc}^{Ttre}$, $K_{i,pal}^{Ttre}$, $K_{i,pal}^{Tglc}$, and k). A value of 7 mM (10) was used for the inhibition constant of glucose for trehalase activity ($K_{i,glc}^{trehalse}$).

The model provided a good fit to the experimental data, as shown by the excellent match between the simulated and experimental values (Fig. 5). The best-fit parameters are shown in Table 2; additionally, a value of 2.2 ± 0.33 $\times 10^{-3}$/min/mg of protein was obtained for the first-order rate constant of glucose and trehalose exchange through the outer membrane.

Most parameter values showed satisfactory standard deviations; the only exception was the inhibition constant of palatinose for the trehalose transporter (Table 2). This uncertainty resulted from the high palatinose concentration (7.5 mM) relative to K_i; under these conditions any value lower than the

TABLE 2. Apparent and calculated values for the kinetic parameters of trehalose transport, glucose transport, and trehalase activity

Transport or activity	Type of value	K_m (μM)	V_{max} (nmol/min/mg)	K_i	
				Glucose (μM)	Palatinose (mM)
Trehalose transport	Apparent	0.42 ± 0.04	0.56 ± 0.02	43 ± 6	0.4 ± 0.14
	Model fit	0.11 ± 0.03	0.39 ± 0.02	27 ± 4	0.002 ± 0.05
Glucose transport	Apparent	69 ± 6	52 ± 1		14 ± 2
	Model fit	46 ± 3	48 ± 1		16 ± 1
Trehalase activity	Apparent	156 ± 11	21.2 ± 0.4		
	Model fit	118 ± 14	20.9 ± 0.5		

standard deviation (0.05 mM) would result in complete inhibition of trehalose transport.

The best-fit parameters were used to simulate the fate of trehalose as a function of trehalose concentration (Fig. 6). In the low range of trehalose concentrations (micromolar range), this sugar was taken up mainly by the high-affinity trehalose transporter; at higher concentrations, most of the trehalose was processed via trehalase and entered the cell through the glucose transport system. For example, at a trehalose concentration of 100 μM, only 9.8% of the trehalose entered the cell via the specific transporter, while when the concentration of trehalose was 1 μM, the proportion increased to 87%. At an external trehalose concentration of 6.2 μM, equal amounts of trehalose entered the cells via the two systems. A considerable proportion of glucose resulting from the trehalase activity diffused out of the periplasm (60 to 66%). It should be noted that for these simulations the following experimental conditions were used: 0.362 mg of cell protein (total suspension volume, 2 ml) and a time of 2 min after trehalose was supplied.

DISCUSSION

The transport of trehalose in the thermophilic bacterium *R. marinus* was characterized in this study. The presence of a periplasmic trehalase necessitated an integrated analysis of a large set of kinetic data for trehalose and glucose uptake, as well as for trehalase. As our attempts to selectively inhibit trehalase or the glucose transport system were unsuccessful, it was essential to resort to mathematical modeling for interpretation of the experimental data. The data were perfectly reproduced by a model that assumed that there is a single trehalose transport system with very high affinity (K_m = 0.1 μM) in addition to a glucose transport system. Furthermore, the calculated kinetic parameters were within the normal ranges of physiological values. On the experimental side, the detection of intracellular trehalose, taken up from the extracellular medium, strongly supported the hypothesis that there is a specific trehalose transporter. Moreover, additional evidence for the existence of distinct transport systems for glucose and trehalose was obtained from competition assays; the uptake of trehalose in the micromolar concentration range was strongly inhibited by all sugars examined, while the transport of glucose was not affected.

As expected, the values of the kinetic parameters calculated using the model were different from those obtained by direct fitting of the experimental data to Michaelian functions (Table 2), since this method disregards the equilibrium between the extracellular and periplasmic pools of glucose and trehalose, as well as the activity of trehalase. The model was validated by simulating the inhibitory effects of glucose (and palatinose) on trehalose transport, as well as the effects of trehalose (and palatinose) on glucose transport. Naturally, the experimental

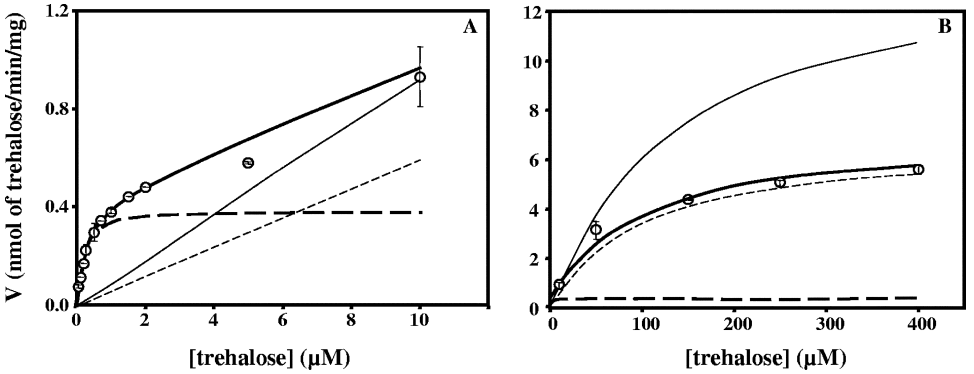

FIG. 6. Fate of trehalose in *R. marinus* as predicted by the model at low concentrations (A) and at high concentrations (B). The lines indicate the rate of trehalose uptake through the trehalose transport system (thick dashed line) and through the glucose transport system (thin dashed line), the diffusion of glucose out of the periplasm (thin solid line), and trehalose uptake predicted by the model (thick solid line). ○, experimental data for trehalose uptake. The fate of trehalose was calculated using 0.362 mg of cell protein (total volume of the suspension, 2 ml) and a time of 2 min after trehalose was supplied.

data were not used for the model fit. The agreement between experimental and calculated data was very good (correlation coefficient, 0.997), showing the reliability of the proposed model (Fig. 3).

We propose that *R. marinus* possesses a high-affinity, low-capacity transporter for trehalose which is distinct from the glucose transporter. The assumption that there are two trehalose transporters resulted in no significant improvement in the quality of the fit; hence, there is no justification for increasing the degrees of freedom of the model. On the other hand, the similarity of the competition patterns observed for glucose and trehalose uptake in the upper range of concentrations (Fig. 3B and C) corroborates the conclusion that there is a single trehalose transport system. It is worth noting that the model discriminates transport systems on the basis of the dissimilarity of their kinetic properties.

Intriguingly, for the high range of trehalose concentrations (on the order of 100 μM) the model predicts that a substantial proportion (around 60%) of glucose in the periplasm diffuses into the external medium. A plausible explanation for this involves the relatively low affinity and low capacity of the glucose transport system of *R. marinus*, an organism that thrives in habitats essentially devoid of monosaccharides. In fact, the glucose transport capacity of *E. coli* or *Lactococcus lactis*, a typical glucose-utilizing organism, is about 1 order of magnitude higher (7, 23). Therefore, the glucose transport system of *R. marinus* is unable to take up glucose efficiently, and part of the glucose produced in the periplasm by the action of trehalase is released.

It appears that the high-affinity trehalose transport system is used to scavenge trehalose when this sugar is scarce in the medium. On the other hand, when higher concentrations are present, the uptake of trehalose is considerably enhanced due to the action of the periplasmic trehalase and import of the resulting glucose via the specific transport system. Thus, the low capacity of the trehalose transporter of *R. marinus* (0.39 nmol/min/mg of protein) is counterbalanced by the activity of the periplasmic trehalase, but naturally the importance of this contribution is restricted to concentrations in the range of or greater than the K_m value of the enzyme (118 μM).

The capacity of the trehalose transporter in *R. marinus* is 1 order of magnitude lower than that of trehalose transporters in other thermophilic and hyperthermophilic prokaryotes (18, 25). As the genomes of thermophiles and hyperthermophiles available in databanks lack homologs of trehalase genes, it appears that the strategy used by *R. marinus* to take up trehalose is unique at least among organisms from hot environments.

Trehalose is frequently used as a compatible solute both in mesophiles and in thermophiles and hyperthermophiles, but only minor amounts of this sugar accumulate in *R. marinus* (19). The expression of the trehalose transporter decreased with elevated salinity (4% NaCl), whereas trehalose-6-phosphate synthase, the first enzyme in the usual pathway for trehalose synthesis, was strongly induced under the same conditions (data not shown), a regulation pattern resembling that of *E. coli* (2).

Some effort was made to determine the nature of the trehalose transport system in *R. marinus*, but a definite conclusion cannot be put forward at this stage. The weak inhibition caused by NaF suggests that the PTS is not involved. In fact, the occurrence of PTS in thermophiles and hyperthermophiles is extremely rare; the only exception is the thermophilic bacterium *Bacillus stearothermophilus*, which possesses PTSs for mannitol and cellobiose (8, 12). On the other hand, all thermophilic and hyperthermophilic organisms examined thus far transport trehalose via ABC transport systems (5, 9, 11, 18, 24, 25). The strong reduction in trehalose transport induced by arsenate in *R. marinus* is consistent with this type of system. BLAST searches performed with the genome of this bacterium using the amino acid sequences of several trehalose binding proteins revealed the presence of one gene encoding a protein with 30% identity to trehalose binding proteins of *Thermotoga maritima* and 23% identity with the trehalose binding protein of *Thermoanaerobacter ethanolicus* (G. Hreggvidsson and J. Kristjánson, Prokaria, personal communication). The corresponding gene was cloned and expressed in *E. coli*, but we did not detect binding activity in radiolabeled assays using trehalose, glucose, maltose, or maltotriose as a putative substrate. Evidence for binding was not obtained even after a unfolding/refolding step to remove potential endogenous substrates. Therefore, the presence of an ABC transporter could not be confirmed. On the other hand, the elimination of trehalose uptake (as well as glucose uptake) by the protonophore CCCP suggests that proton motive force (PMF) systems are involved. A PMF transport system for trehalose has been characterized in the mesophile *Saccharomyces cerevisiae* (21), and uptake of glucose coupled to ion gradients is frequently found (14); in thermophiles and hyperthermophiles, however, only the PMF system for glucose transport in *Thermotoga neapolitana* has been characterized (6). A final conclusion about the nature of the trehalose transport in *R. marinus* must await the development of genetic tools and the construction of suitable strains.

In conclusion, we propose that *R. marinus* possesses distinct transport systems for trehalose and glucose and uses two routes for trehalose assimilation; in trehalose-poor media this sugar is taken up via a high-affinity, low-capacity trehalose transporter, whereas at high concentrations trehalose was primarily hydrolyzed to glucose in the periplasm, with subsequent uptake of this sugar via a specific transport system. The involvement of the periplasmic trehalase provides a means to overcome the low capacity of the trehalose transporter in this organism.

ACKNOWLEDGMENTS

This work was funded by European Commission contract COOP-CT-2003-508644 and by Fundação para a Ciência e a Tecnologia and FEDER, Portugal, grant POCI/BIA-MIC/59310/2004. C.J. and L.L.F. acknowledge FCT for providing research grants SFRH/BD/10572/2002 and SFRH//BPD/26902/2006.

REFERENCES

1. **Alfredsson, G. A., J. K. Kristjansson, S. Hjorleifsdottir, and K. O. Stetter.** 1988. *Rhodothermus marinus*, gen nov, sp nov, a thermophilic, halophilic bacterium from submarine hot springs in Iceland. J. Gen. Microbiol. **134:** 299–306.
2. **Boos, W., U. Ehmann, H. Forkl, W. Klein, M. Rimmele, and P. Postma.** 1990. Trehalose transport and metabolism in *Escherichia coli*. J. Bacteriol. **172:** 3450–3461.
3. **Bradford, M. M.** 1976. A rapid and sensitive method for the quantitation of microgram quantities of protein utilizing the principle of protein-dye binding. Anal. Biochem. **72:**248–254.
4. **Elbein, A. D., Y. T. Pan, I. Pastuszak, and D. Carroll.** 2003. New insights on trehalose: a multifunctional molecule. Glycobiology **13:**17–27.

5. **Elferink, M. G., S. V. Albers, W. N. Konings, and A. J. Driessen.** 2001. Sugar transport in *Sulfolobus solfataricus* is mediated by two families of binding protein-dependent ABC transporters. Mol. Microbiol. **396:**1494–1503.
6. **Galperin, M. Y., K. M. Noll, and A. H. Romano.** 1996. The glucose transport system of the hyperthermophilic anaerobic bacterium *Thermotoga neapolitana*. Appl. Environ. Microbiol. **62:**2915–2918.
7. **Gosset, G.** 2005. Improvement of *Escherichia coli* production strains by modification of the phosphoenolpyruvate:sugar phosphotransferase system. Microb. Cell Fact. **4:**14.
8. **Henstra, S. A., B. Tolner, R. H. ten Hoeve Duurkens, W. N. Konings, and G. T. Robillard.** 1996. Cloning, expression, and isolation of the mannitol transport protein from the thermophilic bacterium *Bacillus stearothermophilus*. J. Bacteriol. **178:**5586–5591.
9. **Jones, C. R., M. Ray, K. A. Dawson, and H. J. Strobel.** 2000. High-affinity binding and transport by the thermophilic anaerobe *Thermoanaerobacter ethanolicus* 39E. Appl. Environ. Microbiol. **66:**995–1000.
10. **Jorge, C. D., M. M. Sampaio, G. O. Hreggvidsson, J. K. Kristjanson, and H. Santos.** 2007. A highly thermostable trehalase from the thermophilic bacterium *Rhodothermus marinus*. Extremophiles **11:**115–122.
11. **Koning, S. M., W. N. Konings, and A. J. Driessen.** 2002. Biochemical evidence for the presence of two α-glucoside ABC-transport systems in the hyperthermophilic archaeon *Pyrococcus furiosus*. Archaea **1:**19–25.
12. **Lai, X., and L. O. Ingram.** 1993. Cloning and sequencing of a cellobiose phosphotransferase system operon from *Bacillus stearothermophilus* XL-65-6 and functional expression in *Escherichia coli*. J. Bacteriol. **175:**6441–6450.
13. **Nunes, O. C., M. M. Donato, and M. S. da Costa.** 1992. Isolation and characterization of *Rhodothermus* strains from S. Miguel, Azores. Syst. Appl. Microbiol. **15:**92–97.
14. **Pao, S. S., I. T. Paulsen, and M. H. Saier, Jr.** 1998. Major facilitator superfamily. Microbiol. Mol. Biol. Rev. **62:**1–34.
15. **Sampaio, M. M.** 2005. Engineering *Escherichia coli* for the synthesis of mannosylglycerate, a solute widely distributed in (hyper)thermophiles: transport, metabolism and physiological role. Ph.D. thesis. Universidade Nova de Lisboa, Oeiras, Portugal.
16. **Santos, H., and M. S. da Costa.** 2002. Compatible solutes of organisms that live in hot saline environments. Environ. Microbiol. **4:**501–509.
17. **Santos, H., P. Lamosa, N. Borges, T. Q. Faria, and C. Neves.** 2007. The physiological role, biosynthesis and mode of action of compatible solutes from (hyper)thermophiles, p. 86–103. *In* C. Gerday and N. Glansdorff (ed.), Physiology and biochemistry of extremophiles. ASM Press, Washington, DC.
18. **Silva, Z., M. M. Sampaio, A. Henne, A. Böhm, R. Gutzat, W. Boos, M. S. da Costa, and H. Santos.** 2005. The high-affinity maltose/trehalose ABC transporter in the extremely thermophilic bacterium *Thermus thermophilus* HB27 also recognizes sucrose and palatinose. J. Bacteriol. **187:**1210–1218.
19. **Silva, Z., N. Borges, L. O. Martins, R. Wait, M. S. da Costa, and H. Santos.** 1999. Combined effect of the growth temperature and salinity of the medium on the accumulation of compatible solutes by *Rhodothermus marinus* and *Rhodothermus obamensis*. Extremophiles **3:**163–172.
20. **Silva, Z., S. Alarico, A. Nobre, R. Horlacher, J. Marugg, W. Boos, A. I. Mingote, and M. S. da Costa.** 2003. Osmotic adaptation of *Thermus thermophilus* RQ-1: lesson from a mutant deficient in synthesis of trehalose. J. Bacteriol. **185:**5943–5952.
21. **Stambuk, B. U., P. S. Araujo, A. D. Panek, and R. Serrano.** 1996. Kinetics and energetics of trehalose transport in *Saccharomyces cerevisiae*. Eur. J. Biochem. **237:**876–881.
22. **Stock, J. B., B. Rauch, and S. Roseman.** 1977. Periplasmic space in *Salmonella typhimurium* and *Escherichia coli*. J. Biol. Chem. **252:**7850–7861.
23. **Thompson, J.** 1987. Sugar transport in the lactic acid bacteria. p. 13–38. *In* J. Reizer and A. Peterkofsky (ed.), Sugar transport and metabolism in Gram-positive bacteria. Ellis Horwood Ltd., Chichester, England.
24. **Wassenberg, D., W. Liebl, and R. Jaenicke.** 2000. Maltose-binding protein from the hyperthermophilic bacterium *Thermotoga maritima*: stability and binding properties. J. Mol. Biol. **295:**279–288.
25. **Xavier, K. B., L. O. Martins, R. Peist, M. Kossmann, W. Boos, and H. Santos.** 1996. High-affinity maltose/trehalose transport system in the hyperthermophilic archaeon *Thermococcus litoralis*. J. Bacteriol. **178:**4773–4777.
26. **Zipper, C., M. Bunk, A. J. Zehnder, and H. P. Kohler.** 1998. Enantioselective uptake and degradation of the chiral herbicide dichlorprop [(RS)-2-(2,4-dichlorophenoxy)propanoic acid] by *Sphingomonas herbicidovorans* MH. J. Bacteriol. **180:**3368–3374.